Supplementary Note 1. Electrochemical experiment
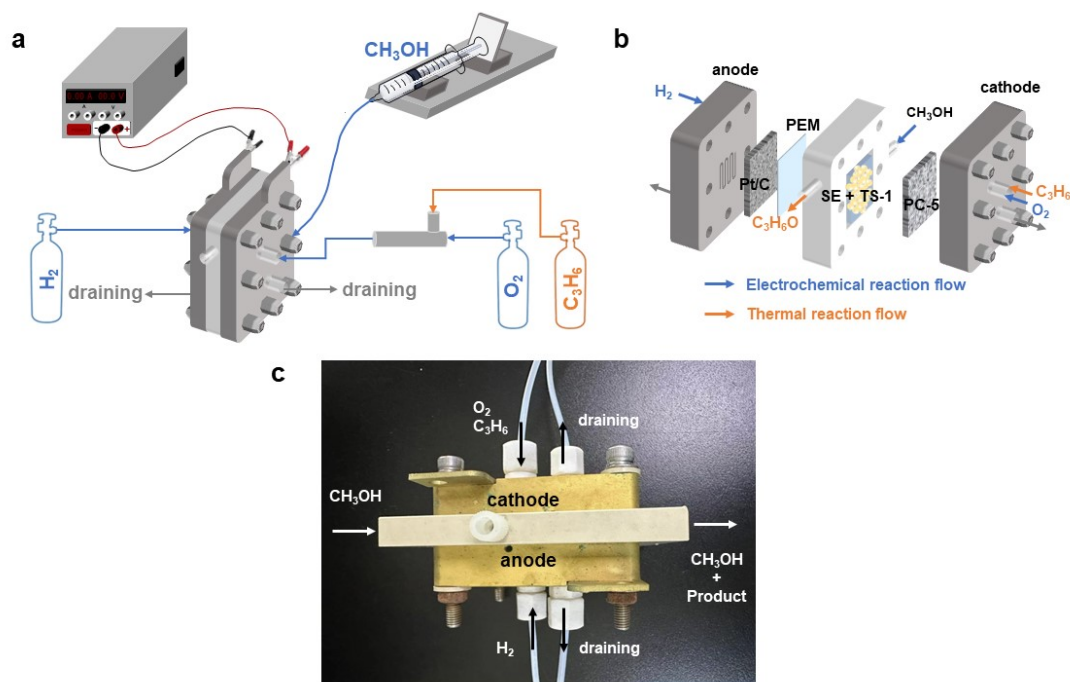

Figure S1. a) and b) schematic and c) physical diagrams of the device.
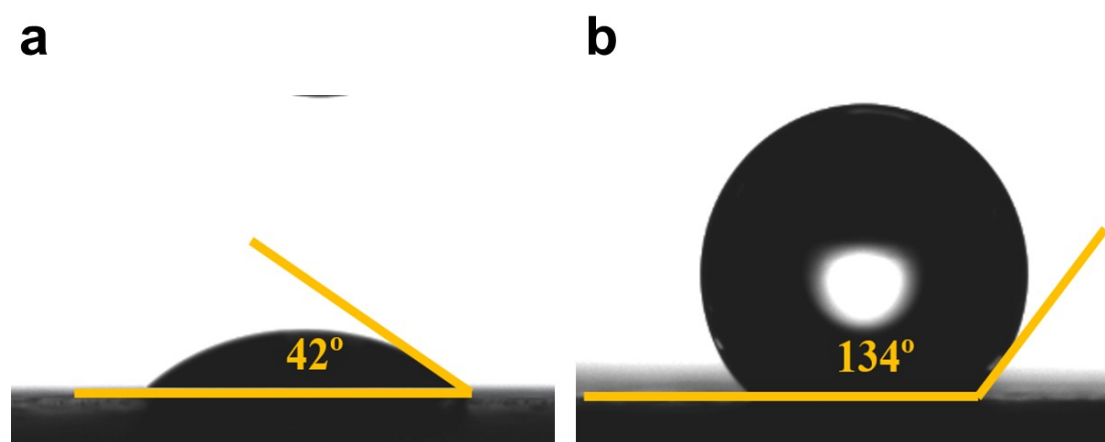

Figure S2. Contact angle of electrode surface a) before and b) after modification.
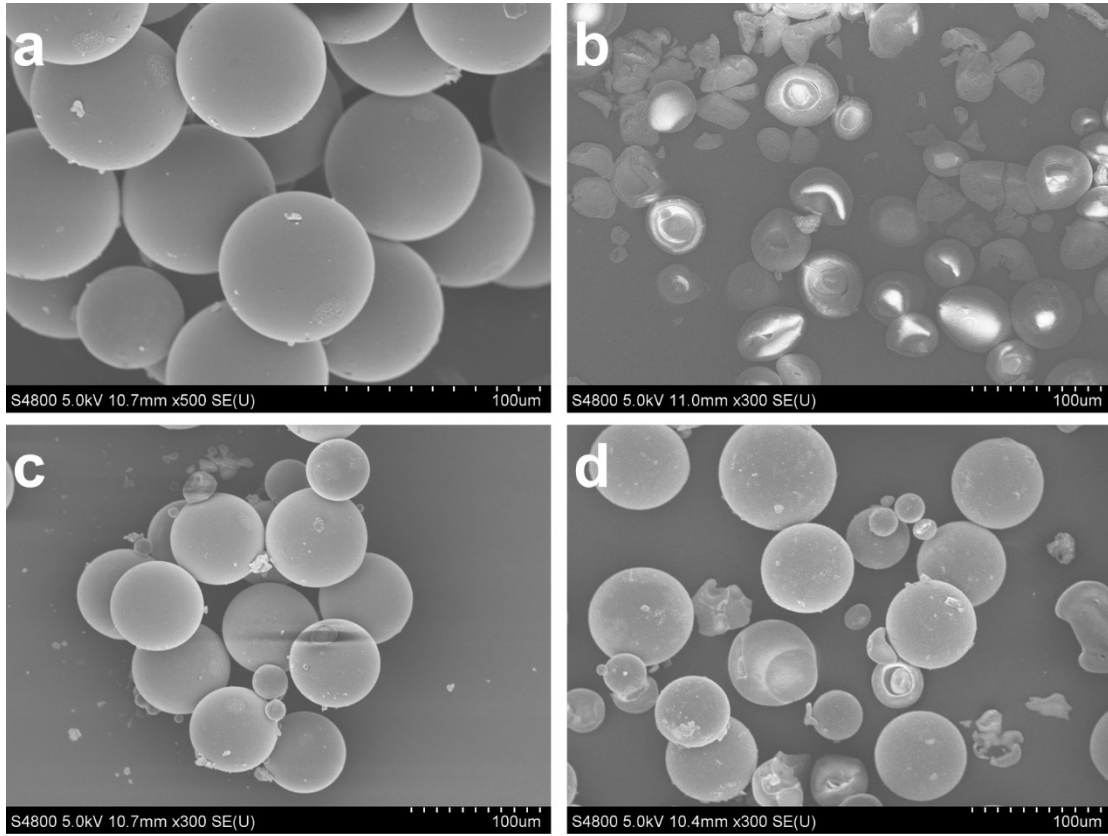
Figure S3. Scanning electron microscopy of a) solid electrolytes, b) titanium silicon molecular sieves, and c, d) fillers.
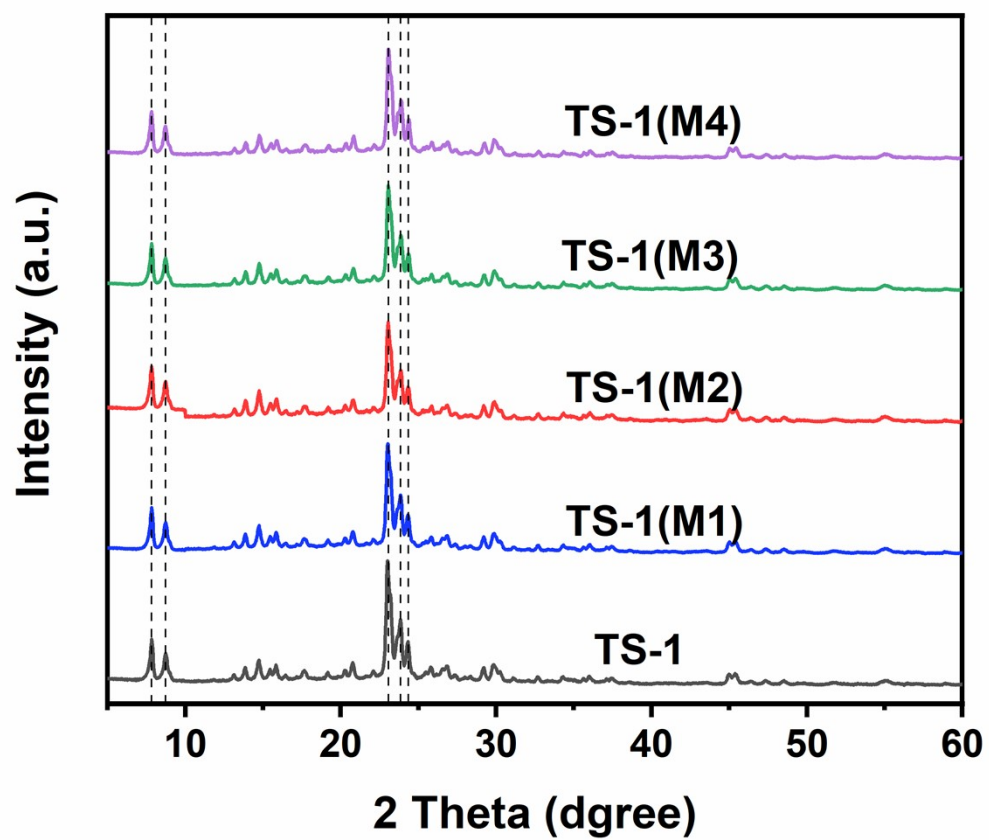
Figure S4. XRD of TS-1 and modified samples.
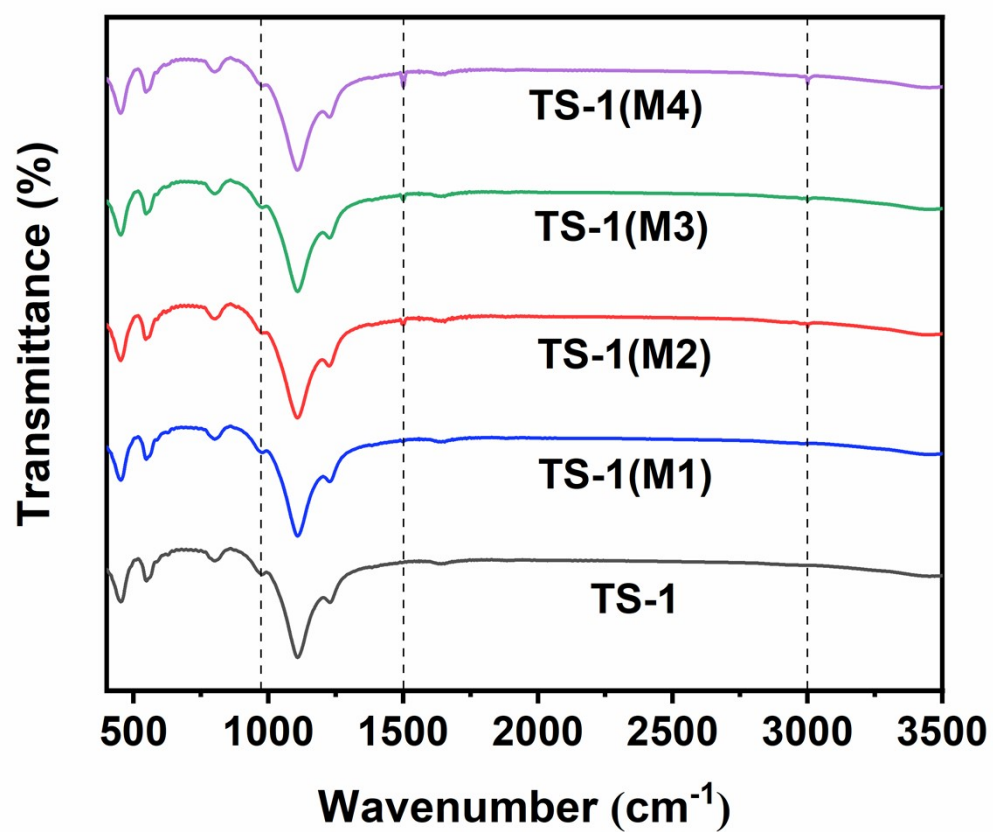
Figure S5. FTIR of TS-1 and modified samples.

Table S1. Specific surface area, pore size, and pore volume of electrocatalysts.

Catalyst	O %	O_I %	O_{II} %	O_{III} %	H_2O_2 selectivity %
PC-20	12.12	61.87	30.22	7.54	96.44
PC-10	10.20	72.65	19.66	7.68	95.71
PC-5	8.72	81.25	14.06	4.69	88.06
PC-2	5.58	83.65	11.07	6.32	72.42

Supplementary Note 2. Computation results

a

b

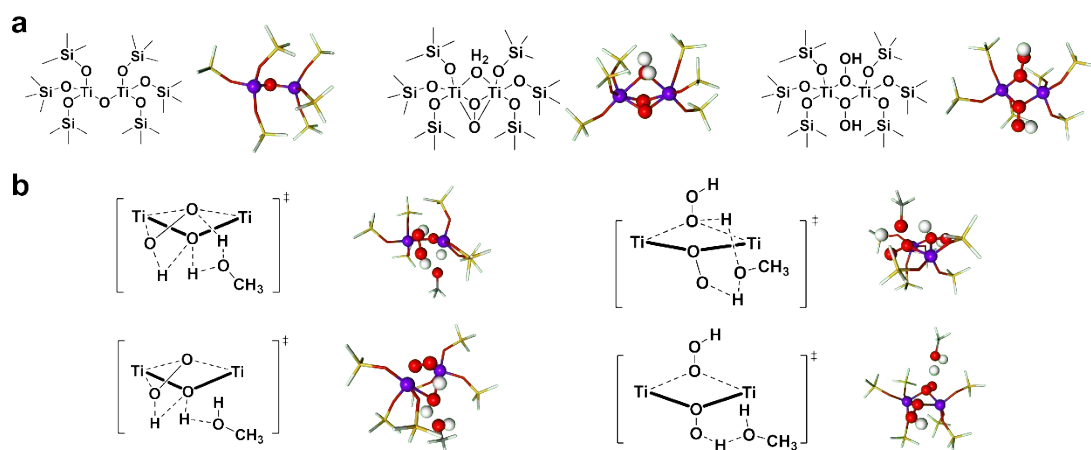**Figure S6.** Computation configurations of (a) intermediates and (b) transition state. Red balls, water balls and purple balls are presented for oxygen atoms, hydrogen atoms and titanium atoms, respectively.

a

$E_{HOMO,H2O2} = -7.97$ eV $E_{HOMO,OOH^-} = 1.54$ eV

b

$E_{O-H-1,H2O2} = 3.73$ eV
$E_{O-H-2,H2O2} = 3.92$ eV

$E_{O-H,OOH^-} = 2.63$ eV
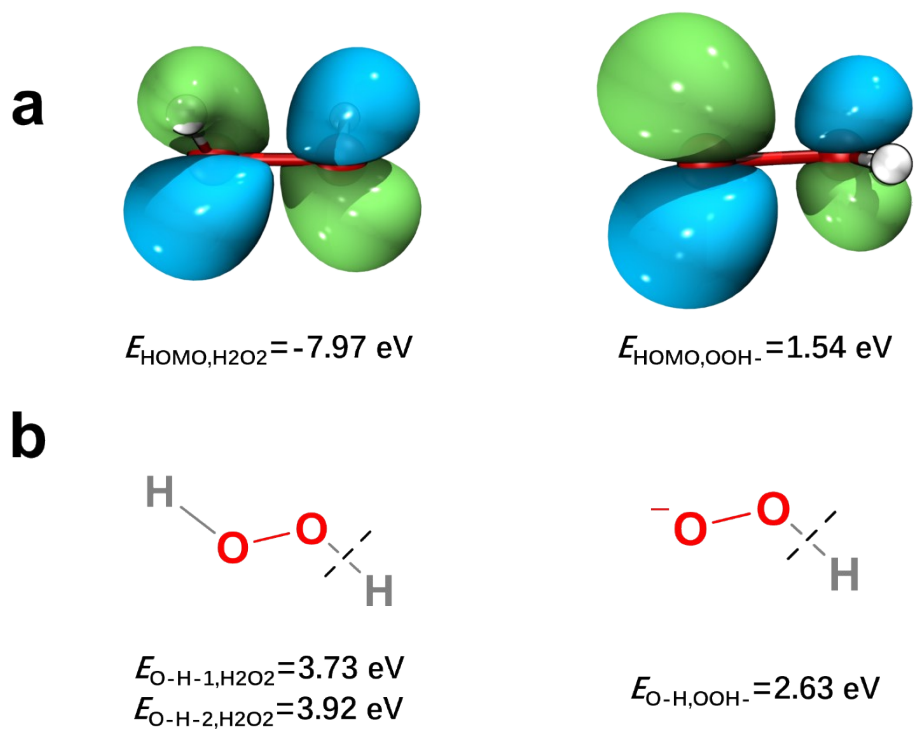
Figure S7. (a) HOMO energy and (b) O-H bonds energy of H_2O_2 and OOH^-.

As shown in Figure S7, a higher HOMO energy of OOH- suggested that its electrons can more readily donate to the Lewis acid site Ti, thereby enhancing the interaction with TS-1 and facilitating the transport of OOH- species from the solid electrolyte to TS-1. Additionally, a lower O-H bond energy of OOH- indicated that the O-H bond in H2O2 was easy to break, thereby facilitating proton transfer.

Supplementary Note 3. Techno-economic analysis (TEA) and life-cycle assessment (LCA)

2.1 Electrochemical PO production process

The electrochemical PO production process has been developed with the aim of generating 100,000 tons of PO annually, operating for 8,000 hours per year. Overall, the electrochemical PO production process encompasses three main stages: PO synthesis, PO separation and purification, and the working liquid cycle (methanol), as depicted in Figure S8. The design of the PO synthesis unit is based on parameters derived from electrochemical PO synthesis experiments, specifically reactions (1-4). The PO separation and purification, and the working liquid cycle are implemented using the Aspen Plus software, employing the RadFrac model and the Sensitivity Analysis module for parameter optimization. The entire process is modeled within the Aspen Plus software, with the optimized model parameters detailed in Table S2. The mass balance results are outlined in Table S3. These results serve as the basis for subsequent TEA and LCA of the electrochemical PO production process.
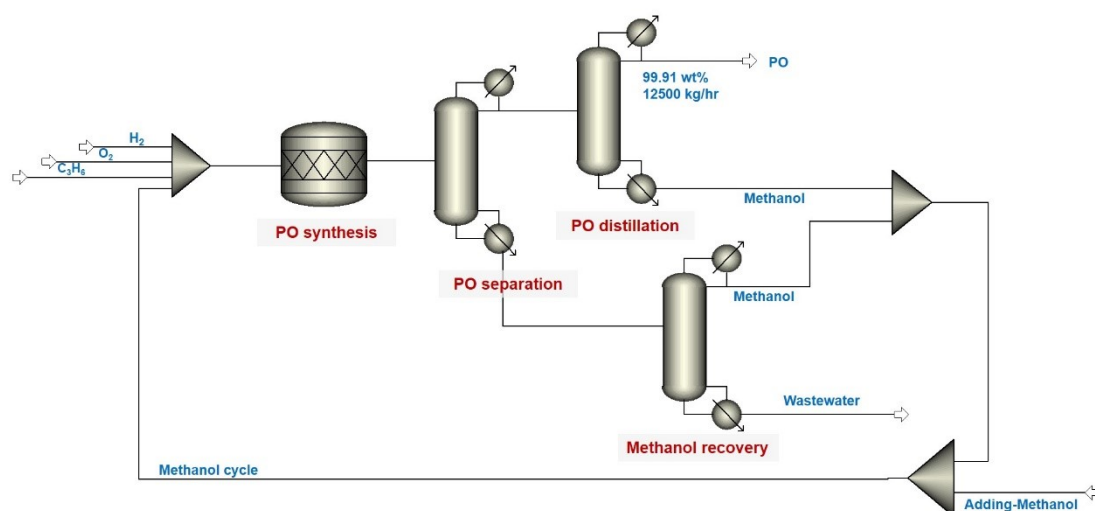

Figure S8. Electrochemical PO production process.

$$O_2 + H_2 = H_2O_2 \tag{R1}$$

$$H_2O_2 + C_3H_6 = C_3H_6O + H_2O \tag{R2}$$

$$C_3H_6O + H_2O = C_3H_8O_2 \tag{R3}$$

$$C_3H_6O + CH_4O = C_4H_{10}O_2 \tag{R4}$$

where the reactions (R1-R2) are designed to achieve a conversion rate of 100% each based on experimental results, the conversion rates in reaction (R3) and reaction (R4) are 3.80% and 1.00%, respectively.

Table S2. Specification in each unit.

Units	Models and Parameters
PO synthesis	RStoic model, 45 °C, 1 bar Parameters are set according to the experiment, see reactions (1-4)
PO separation	RadFrac model, NG: 36; RR: 3.5; FS: 10 Distillate to feed ratio: 0.2 (mass)
PO distillation	RadFrac model, NG: 16; RR: 1.5; FS: 7 Distillate to feed ratio: 0.76 (mass)
Methanol recovery	RadFrac model, NG: 14; RR: 1.3; FS: 7 Bottoms to feed ratio: 0.075 (mass)

*The process simulation was performed using Aspen Plus V14, with the NRTL (Non-Random Two-Liquid) thermodynamic model employed for property calculations. In the simulation, NG represents the number of stages, RR denotes the reflux ratio (in mole), and FS represents the feed stage.

Table S3. Inputs and outputs of process.

Inputs, kg/hr		Outputs, kg/hr	
Hydrogen	457.99	PO	12500 (99.98 wt%)
Oxygen	7269.82	Wastewater	4934.21
Propylene	9560.31	[a] RE-methanol	64802.63 (99.98 wt%)
Methanol	64948.72		

2.1.1. Energy analysis

The energy consumption consists of two parts. On one hand, there is the electrical consumption of the electrochemical reactor, which can be calculated based on experimental results. On the other hand, there is the energy consumption associated with the separation process, which can be calculated using Aspen Plus software.

(1) Energy consumption in electrochemical reactor

According to the electrochemical PO production mechanism, the PO production is a 2-electron reaction, that is, producing 1 mol of PO will transfer 2 mol of electrons, and the electron transfer contribution comes from reactions (R1). Note that the reactions (R2) do not involve electron transfer in the electrochemical reaction.

Thus, the charge transfer number for the electrochemical PO production process, which produces 12500 t/hr of PO, was calculated by equation (1).

$$Q = \frac{nNF}{\eta} = \frac{mNF}{\eta M_{PO}} \tag{1}$$

where Q is the total charge, F is the Faraday's constant ($F=96485$ C/mol), η is the Faradaic efficiency ($\eta=1$), and N takes the value 2 since propylene oxidation to PO is a two-electron transfer process. Additionally, n, m, and M_{PO} are the mole number, mass, and molar mass of PO ($M_{PO}=58$ g/mol).

Therefore, the electrical consumption of the electrochemical reactor can be obtained through equations (2-4). Firstly, to determine the current required to sustain the electrochemical PO production process, equation (2) was utilized to calculate the current.

$$I = \frac{Q}{t} \tag{2}$$

where I is the current, that is, the number of charges flowing through the cross section per unit time, A; t is the time, s.

Then, the power of the electrochemical reactor is defined by equation (3).

$$P = IU \tag{3}$$

where P is the power of the electrochemical reactor, W; U is the voltage of the electrode sheet, 1.5 V.

Finally, the total annual electrical consumption of the electrochemical reactor is calculated using equation (4).

$$W = Pt_{PO} \tag{4}$$

where W is the power consumption of the electrochemical reactor, kWh; t_{PO} is the total operating time of the year, 8000 hours.

After the calculation, the annual power consumption of the electrochemical reactor is determined to be 138627873.56 kWh. Detailed results are presented in Table S4.

Table S4. Energy calculation of the electrochemical reactor.

Projects	Values	Units
Q	41588362.07	C
I	11552.32	A
P	17328.48	kW
W	138627873.60	kWh

(2) Energy consumption in separation process

The energy consumption associated with the separation process, including the PO separation and purification and the methanol recovery of the three towers, was calculated using Aspen Plus software, as illustrated in Table S5.

Table S5. Energy inputs in separation process.

Projects	Values	Units
PO separation	388442987.34	MJ
PO distillation	122081678.99	MJ
Methanol recovery	1274047510.54	MJ

Therefore, the total energy consumption of the electrochemical PO production process is equal to the sum of the energy consumption in the electrochemical reactor and the energy consumption in the separation process, as shown in equation (5).

$$E_{total} = W + E_{sep} \tag{5}$$

where E_{total} is the total energy consumption of the electrochemical PO production process; E_{sep} is the energy consumption in the separation process.

The total energy consumption amounted to 2283632521.69 MJ, Figure S9 illustrates the contribution of each unit to the overall energy consumption. The main energy consumption comes from the methanol recovery and the electrochemical reactor, accounting for 55.79% and 21.85%, respectively. It is worth noting that the energy supply forms are different for four units. The electrochemical reactor primarily

relies on electrical energy supply, while the separation process utilizes natural gas combustion for energy supply.
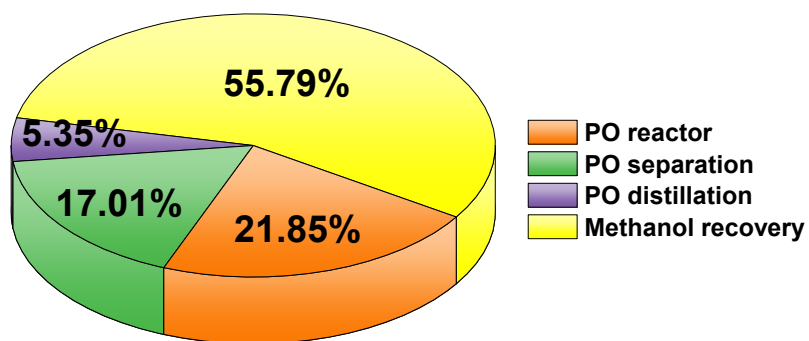

Figure S9. Contribution of each unit to energy consumption.

2.1.2. Techno-economic analysis

The total cost includes five components, as illustrated in Figure S10. We will now perform an example Techno-economic analysis (TEA) calculation. Below is a comprehensive list of the assumptions made for the analysis:
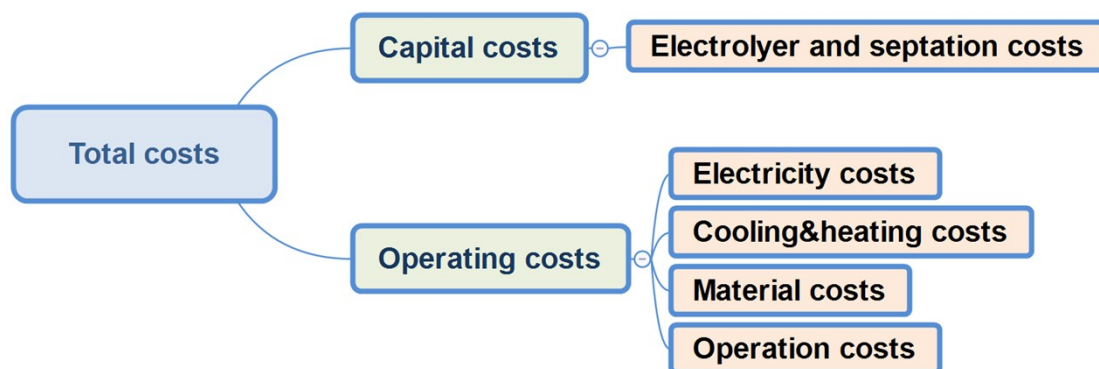

Figure S10. Model used for calculating the techno-economic analysis.

1. To calculate electrolyser capital costs, we assume a cost of $1000 per m^2 of electrolyser according to the Table S6. The plant will have a lifetime of 30 years. Separations equipment capital costs will be assumed to be 10 % of the electrolyser capital costs.

Table S6. The market prices of raw materials used for electrolyser[1].

Items	Price
Carbon black ($/kg)	10
Stainless steel mesh ($/m²)	30
PTFE 60% dispersion ($/kg)	10
DSA ($/m²)	450
Cation exchange membrane ($/m²)	180-2400
Electrolyser capital costs ($/m²)	1000

2. Feedstock costs are variable, including electricity, hydrogen, propylene, and other inputs. Additionally, specific costs will be assumed as shown in Table S7.

Table S7. Cost list for mainly feedstock.

Items	unit cost	Units
Electricity[1]	0.063	$/kWh
Hydrogen[2]	1124	$/t
Propylene[2]	896.4	$/t
Process water[2]	0.535	$/t
Cooling water[3]	1.5	$/t
Oxygen[3]	60	$/t
Methanol[2]	360	$/t

3. Separation equipment costs consist of 3 components, including three distillation towers of PO separation, PO distillation, and methanol recovery. Their combined cost is assumed to be 10% of electrolyser cost.

4. Cooling&heating in the separation process are assumed to be 30% of electricity costs.

5. Operation costs are assumed to be 10% of the capital costs.

6. The electrochemical PO production process is designed for an annual production of 100000 tons. The plant operates for 8000 hours per year, resulting in a PO production rate of 12500 kg/hr.

7. The faradaic efficiency to produce PO is 100%. The total operating voltage of the cell is 1.5 V, and the total operating current density is 200 A/m².

Next, we will calculate each of the 5 components for a conventional year of operation, see equations (6-15).

(1) Capital costs

We first calculate the electrolyser cost. Based on the current required and the assumed operating current density of 200 A/m² we can calculate the area of electrolyser needed, equation (6):

$$Area\ of\ electrolyser = \frac{Q}{current\ density} \tag{6}$$

Thus, further calculations can be performed to determine the electrolyser cost, separation cost, and capital costs per ton of PO, equations (8-10). The results of this calculation are listed in Table S8.

$$Electrolyser\ cost = Electrolyser\ area \times electrolyser\ cost\ per\ area \tag{7}$$
$$Separation\ cost = 0.1 \times electrolyser\ cost \tag{8}$$
$$Equipment\ cost = separation\ cost + electrolyser\ cost \tag{9}$$
$$Capital\ costs = \frac{equipment\ cost \times Capital\ recovery\ factor}{Total\ PO\ production} \tag{10}$$

where the capital recovery factor can be calculated using equation (11).

$$Capital\ recovery\ factor = \frac{Discount\ rate \times (1 + Discount\ rate)^{Lifetime}}{(1 + Discount\ rate)^{Lifetime} - 1} \tag{11}$$

where the Discount rate is 0.1 and the Lifetime is 30 years.

Table S8. Capital cost results.

Items	$/t-PO
Electrolyser cost	220.58
Separation cost	22.06
Capital costs	242.64

(2) Electricity costs

The electrical consumption of the electrochemical reactor, normalized by the mass of PO produced, can be calculated using equation (12).

$$Electricity\ cost = \frac{Electricity\ use\ \times\ Cost\ per\ kWh}{Total\ PO\ production}$$
$$= \frac{138627873.60\ kWh \times 0.063\ \$/kWh}{100000\ t} = 87.34\ \$/t$$

(12)

(3) Cooling&heating costs

The cooling and heating utility costs can be calculated as 30% of the electricity costs, see equation (13).

$$Separation\ costs = Electricity\ cost\ \times\ 0.3$$
$$= 87.34\ \$/t \times 0.3 = 26.20\ \$/t$$

(13)

(4) Material costs

The material costs, which involve the feedstocks in the overall process, can be calculated using equation (14). The results of this calculation are listed in Table S9.

$$Material\ costs = \frac{Feedstock\ cost_i \times\ mass\ value_i}{Total\ PO\ production}$$

(14)

Table S9. Material costs for mainly feedstock.

Inputs	Values (t/year)	Costs ($/t-PO)
Hydrogen	3663.91	41.18
Oxygen	58158.55	34.90
Propylene	76482.52	685.59
Methanol	1168.70	4.21
Material costs		765.87

(5) Operation costs

The operation costs are assumed to be 10% of the capital costs and are calculated using equation (15).

$$Operation\ costs = 0.1 \times Capital\ costs \qquad (15)$$
$$= 0.1 \times 242.64\ \$/t = 24.26\ \$/t$$

The TEA results found that the cost per ton of PO is \$1146.32. The major contributions to the cost come from material costs and capital costs, especially material costs which account for 66.81% of the total cost, mainly due to the high cost of propylene, Figure S11.
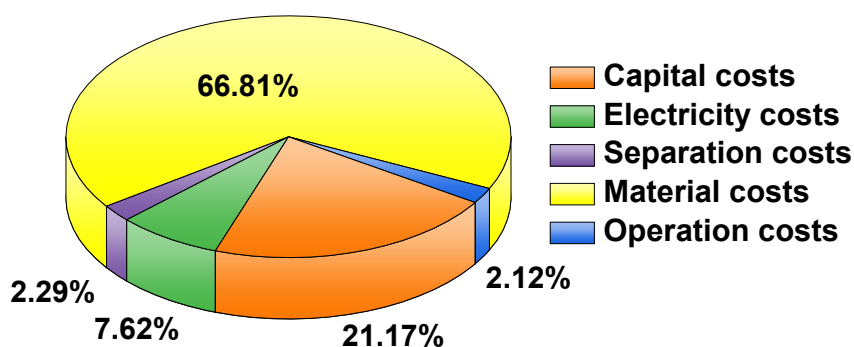

Figure S11. Contribution of each component to costs.

Since 2020, the price of PO in China has been increasing annually, see Figure S12. Throughout 2021, prices remained elevated until December. As of July 2022, prices have stabilized at around \$1617.65 per ton (data source: https:/ /www.100ppi.com/). Furthermore, it indicates a projected price range for PO between February 2023 and February 2024, with a minimum price of \$1343.75 per ton, a maximum price of \$1584.56 per ton, and an average price of \$1413.18 per ton. In this work, the electrochemical PO production process presented achieves a cost per ton of \$1146.32 for PO, offering certain advantages in the current PO market. In addition, a sensitivity analysis was conducted on the key influencing factors of PO cost as follows.
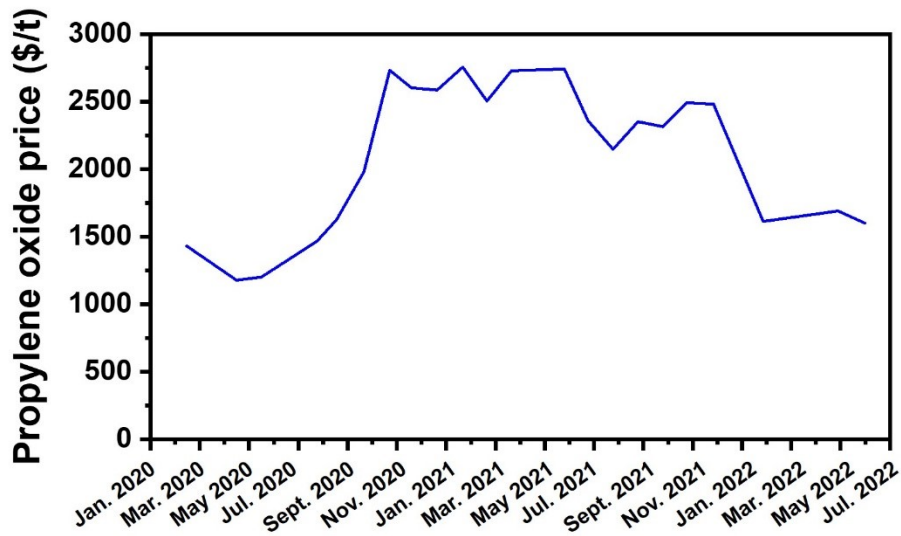
Figure S12. The price trend of PO in China from 2020 to 2022 (www.huaon.com).

(6) Sensitivity analysis

Figure S13 performed a sensitivity analysis on the key influencing factors of PO cost, assessing the impact on PO cost through a 20% increase and decrease for each parameter. In Figure S13, blue represents cost reduction, while red indicates cost increase. For instance, a 20% decrease in electrolyser cost leads to a 4.01% reduction in PO cost. Overall, propylene price, Faradaic efficiency, and electrolyser cost are identified as the primary influencing factors on PO cost.

Figure S13. PO cost sensitivity analysis.

2.1.3. Life cycle assessment

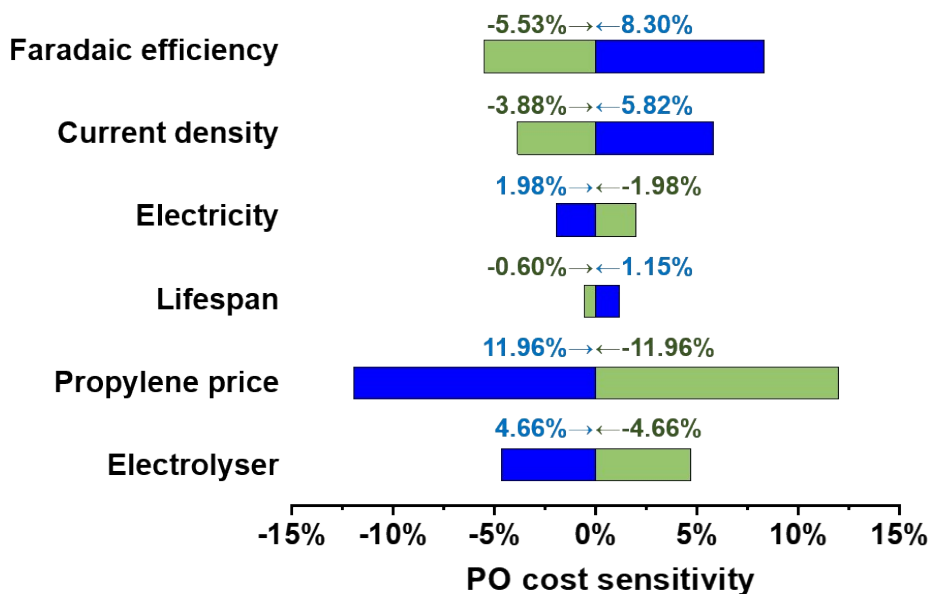The life-cycle assessment (LCA) is a methodology employing category indicators such as global warming potential (GWP) to evaluate sustainability impacts. The objective of this study is to compare the GWP associated with producing 1 kg of PO from the electrochemical PO production process with that of producing 1 kg of PO from the conventional hydrogen peroxide to propylene oxide (HPPO) process for PO production. The system boundary of the study is cradle-to-gate, i.e., the analysis accounted for all stages in the life cycle of production for products, starting from the extraction of raw materials to the production of products, as illustrated in Figure S14.
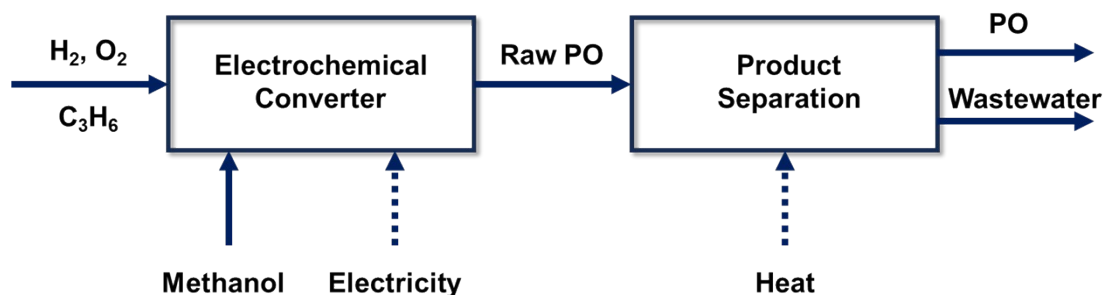
Figure S14. The system boundary of LCA in the electrochemical PO production process.

In our previous work, we integrated LCA with energy chemical software (Aspen Plus) to establish a hybrid LCA method for calculating the carbon footprint of biorefining processes[4-8]. In this study, the background data for the calculation are obtained from China Emission Accounts and Datasets (CEADs) and relevant literature[2, 3, 9], which primarily include emission factors for various energy sources and materials (Table S10). The foreground data are derived from the results of Aspen Plus simulations, mainly comprising mass and energy flow information. The lists of mass and energy involved in the electrochemical PO production have been provided in Sections 1.1 and 1.2 (Supplementary Note 1).

Therefore, the LCA of the electrochemical PO production process can be calculated using equations (16-17).

$$GWP_{total} = \sum_i C_i^u \times GWP_g + \sum_k C_k^m \times GWP_g \tag{16}$$

where the GWP_{total} typically consists of the utility carbon emissions C^u and the material processing carbon emissions C^m. The utility carbon emissions (C^u) are often caused by power, heat, and cooling consumptions in each unit. The material preparation carbon emissions (C^m) originate from production of raw and auxiliary raw materials. And i and k represent different types of utilities and materials, respectively.

The product carbon footprint can be quantified based on a functional unit. The functional unit is kg-prod in this work. The GWP_{PO} is expressed in equation (17):

$$GWP_{PO} = \frac{GWP_{total}}{P_{PO}} \tag{17}$$

where GWP_{total} is the total system CO_2 equivalent calculated from equation (16); and P_{PO} is the amount of PO produced.

Table S10. Emission factors for various energy sources and materials.

Items	High	Low	Unit
Electricity	[a] 0.5703	[b] 0.0108	$kgCO_2e/kWh$
[c] Hydrogen	11.89	0.970	$kgCO_2e/kgH_2$
[d] Propylene	1.470	-0.303	$kgCO_2e/kg\ C_3H_6$
[e] Oxygen	0.128	0.0024	$kgCO_2e/kgO_2$
[f] Methanol	2.971	0.560	$kgCO_2e/kg$ methanol
Natural gas for energy[10]	0.0860	_	$kgCO_2e/MJ$
[g] Wastewater treatment	0.32	0.22	$kgCO_2e/m^3$

[a] The Ministry of Ecology and Environment of the People's Republic of China (2022) has published the average emission factors for the national power grid (https://www.mee.gov.cn/).
[b] Renewable electricity (wind power: 0.0108 $kgCO_2e/kWh$[10]; biomass power: -0.060 $kgCO_2e/kWh$[11])
[c] Hydrogen production methods and their respective carbon footprints are as follows: coal gasification (25.877 $kgCO_2e/kgH_2$[2]), natural gas steam reforming (11.89 $kgCO_2e/kgH_2$[2]), green electricity electrolysis of water (0.970 $kgCO_2e/kgH_2$[2]), and biomass green hydrogen (−5.22 $kgCO_2e/kgH_2$[12]).
[d] Propylene production has varying carbon footprints depending on the source: crude oil cracking (1.470 $kgCO_2e/kgC_3H_6$[2]) and biomass (0.303 $kgCO_2e/kgC_3H_6$[2]).
[e] The power requirements for oxygen production are 0.8064 MJ/kgO_2[13]. When electrical energy is converted into carbon emissions, the value is 0.128 $kgCO_2/kgO_2$, while using renewable electricity results in 0.0024 $kgCO_2/kgO_2$.
[f] Methanol production processes and their associated carbon footprints are as follows: coal-to-methanol (2.971 $kgCO_2e/kg$ methanol[14]), natural gas-to-methanol (0.560 $kgCO_2e/kg$ methanol[15]), and biomass-to-methanol (-0.989 $kgCO_2e/kg$ methanol[16]).

<superscript>g</superscript> Reverse osmosis membrane wastewater treatment has varying carbon footprints based on the electricity source[10]: power grid (0.32 $kgCO_2e/m^3$) and wind power (0.22 $kgCO_2e/m^3$).

Different raw materials and energy sources exert a significant influence on the carbon footprint of electrochemical PO production process. Consequently, we conducted an analysis involving five scenarios based on carbon emission factors from various sources. The description of each scenario is provided in Table S11, and the corresponding results are presented in Table S12.

Table S11. Scenario descriptions.

Scenarios	Descriptions
Scenario 1	Electricity is sourced from the grid, hydrogen is produced through coal gasification, propylene is obtained from petroleum cracking and methanol from coal.
Scenario 2	Electricity is sourced from the grid, hydrogen is produced through natural gas reforming, propylene is obtained from petroleum cracking, and methanol derived from coal.
Scenario 3	Electricity is sourced from wind power, hydrogen is produced through wind power electrolysis of water, propylene is obtained from petroleum cracking, and methanol is derived from coal.
Scenario 4	Electricity is sourced from biomass electricity, hydrogen is produced through biomass hydrogen, propylene is obtained from biomass refining, and methanol is derived from biomass.
Scenario 5	Building upon Scenario 4, the Scenario 5 involves the energy for the separation process being sourced from zero-carbon energy, such as biomass combustion for energy supply.

Table S12. LCA results for different scenarios.

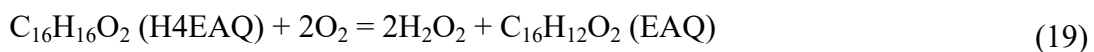| Contributors	Scenario 1	Scenario 2	Scenario 3	Scenario 4	Scenario 5
Electricity (reaction)	1.807	1.807	0.034	-0.190	-0.190
Energy (separation)	1.535	1.535	1.535	1.535	0.000
Feedstocks	2.182	1.641	1.168	-0.433	-0.442
Hydrogen	0.948	0.436	0.036	-0.191	-0.191
Oxygen	0.074	0.074	0.001	0.001	-0.008
Propylene	1.124	1.124	1.124	-0.232	-0.232
Methanol	0.035	0.007	0.007	-0.012	-0.012
<superscript>a</superscript> Wastewater	0.131	0.131	0.090	0.090	0.090
Total ($kgCO_2e/kgPO$)	5.524	4.983	2.737	0.912	-0.632

<superscript>a</superscript> Compared with other contributors, the carbon footprint unit for wastewater process is expressed as $kgCO_2e/tPO$.

Ghanta et al.[17] comparative cradle-to-gate LCA identified significant

environmental impact sources in two technologies: the conventional PO/TBA process (utilizing t-butyl hydroperoxide in the propylene oxide/t-butyl alcohol process) and the HPPO process. The results revealed carbon footprints of 17.805 and 12.990 $kgCO_2e/kgPO$ for the PO/TBA and HPPO processes, respectively. Notably, the electrochemical PO production process in our study demonstrated substantial reductions in carbon footprint, ranging from 0.912 to 5.524 $kgCO_2e/kgPO$ (Table S12). Optimizing the electrochemical PO production process with the use of zero-carbon energy provides potential opportunities for minimizing environmental impact. Results revealed that the process may even achieve negative carbon emissions, with a value of -0.632 $kgCO_2e/kgPO$.

2.2. Conventional PO production process

The conventional PO production process consists of two main components: the anthraquinone process for hydrogen peroxide synthesis and the HPPO process, as illustrated in Figure S15. The conventional PO production process design primarily follows the studies of Liu et al.[18] and Ghanta et al.[17] Firstly, in the anthraquinone process for hydrogen peroxide synthesis, it involves a series of steps such as hydrogenation reaction, oxidation reaction, hydrogen peroxide extraction, concentration of hydrogen peroxide, and working fluid circulation. Specifically, hydrogen reacts with anthraquinone in the working fluid, forming a hydrogenated liquid. After cooling, the hydrogenated liquid undergoes oxidation with the introduced air in the oxidation reactor, producing an oxidized liquid containing hydrogen peroxide (~3 wt%). The oxidized liquid is then extracted with water, obtaining raw hydrogen peroxide (~20 wt%). Following purification and concentration, the final hydrogen peroxide was obtained and reached a commercial concentration of 30 wt%. The working fluid and unreacted raw materials are directly recycled, and hydrogen peroxide is used in the downstream HPPO section. The HPPO section primarily encompasses PO synthesis, PO separation, PO distillation, and the circulation of propylene and methanol. Ultimately, the conventional PO production process achieves an output of 12,500 kg/hr with a purified concentration of 98.63 wt%. Additionally, the primary reactions involved in the entire process are described by equations (18-23). The simulation parameters for the conventional PO production process are provided in Table S13.

$$C_{16}H_{12}O_2 \text{ (EAQ)} + 2H_2 = C_{16}H_{16}O_2 \text{ (H4EAQ)} \tag{18}$$

$$C_{16}H_{16}O_2 \text{ (H4EAQ)} + 2O_2 = 2H_2O_2 + C_{16}H_{12}O_2 \text{ (EAQ)} \tag{19}$$

$$O_2 + H_2 = H_2O_2 \tag{20}$$

$$H_2O_2 + C_3H_6 = C_3H_6O + H_2O \tag{21}$$

$$C_3H_6O + H_2O = C_3H_8O_2 \tag{22}$$

$$C_3H_6O + CH_4O = C_4H_{10}O_2 \tag{23}$$
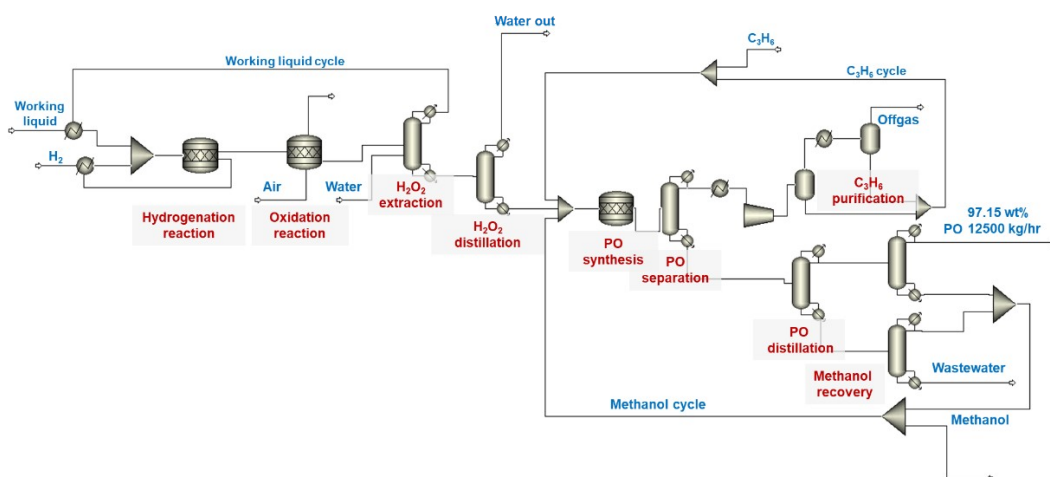
Figure S15. Conventional PO production process.

Table S13. Specification in each unit.

Units	Models and Parameters
Hydrogenation reaction	RStoic, 45 °C, 4 bar The molar conversion rate of hydrogen was set to 0.666.
Oxidation reaction	RStoic, 25 °C, 1 bar The molar conversion rate of H4EAQ is defined as 1.
H_2O_2 extraction	Sep Model
H_2O_2 distillation	RadFrac model, NG: 7; RR: 0.8; FS: 4 Bottoms to feed ratio: 0.7399 (mass).
PO synthesis	RStoic model, 40 °C, 20 bar H_2O_2 decomposes by 10%, and 90% is converted into products. The final molar yield for PO is 85.68%. The mass yields for PG are 3.42% and PM is 0.90%. Reaction temperature: 40 °C; Pressure: 20 bar.
Gas recycle tower	RadFrac model, NG: 10; RR: 2; FS: 5 Distillate to feed ratio: 0.04850 (mass).
Gas compressor	Isentropic, 100 bar
Gas recycle flash	Flash model, 25 °C, 15 bar
Liquid separation	RadFrac model, NG: 22; RR: 2.5; FS: 10 Distillate to feed ratio:0.2250 (mass).
PO distillation	RadFrac model, NG: 10; RR: 3; FS: 5 Distillate to feed ratio: 0.7950 (mass)
Methanol recovery	RadFrac model, NG: 10; RR: 2; FS: 5 Bottoms to feed ratio: 0.5009 (mass).

*The process simulation was performed using Aspen Plus V14, with the NRTL (Non-Random Two-Liquid) thermodynamic model employed for property calculations. In the simulation, NG represents the number of stages, RR denotes the reflux ratio (in mole), and FS represents the feed stage.

2.1.1. Techno-economic analysis

The conventional PO production process has been designed to generate an annual output of 100000 tons of PO, operating for 8000 hours per year. The entire process is simulated and optimized in Aspen Plus V14. Table S14 provides the assumptions for the TEA of the conventional PO production process. In contrast to the TEA of the electrochemical process, both capital investment costs and utility costs for the conventional PO production process are derived from the Aspen Process Economic Analyzer, which is a subroutine software of Aspen Plus, based on the optimized process.

Table S14. Techno-economic analysis assumptions

Projects	Assumptions
Lifespan, year	20
Operating time, hr/year	8000
Capital costs (a*TCR)	
Equipment Cost (EC)	Aspen Plus
Total Installed Cost (TIC)	Aspen Plus
Process plant cost (PPC)	EC+TIC
[a] Discount rate	10%
[b] Total plant cost (TPC)	150% of PPC
[b] Total capital requirement (TCR)	110% of TPC
Capital recovery factor (a)	$a = \dfrac{\text{Discount rate} \times (1 + \text{Discount rate})^{\text{Life}}}{(1 + \text{Discount rate})^{\text{Lifetime}} - 1}$
Operating costs	
Utilities costs	Aspen Plus
[c] Operation cost	30% of TCR
Material costs	Aspen Plus

[a] The real discount rates for the industrial plants found in the literature were 7%–10% for the petrochemicals. In this study a value of 10% was taken[19].

[b] Process plant cost (PPC) comprises equipment and installation costs. Total plant cost (TPC) comprises PPC, engineering fees, and contingencies. Total capital requirement (TCR) comprises TPC, owner costs, and interest during construction[19].

[c] Conventionally, the operation cost includes the plant's operation and maintenance costs, and labor, assumed to be approximately 30% of the TCR based on the literature review[17, 18].

Figure S16 illustrates the breakdown of costs, with detailed TEA results presented in Table S15. The production cost of PO in the traditional process is calculated at $1268.54 per ton, where raw material costs are dominant, accounting for 64.21% of

total costs. Compared with the electrochemical process, utility costs, primarily including cooling water, refrigerant, and steam, consist of 13.5% of the costs, with electricity costs merely 0.46%.
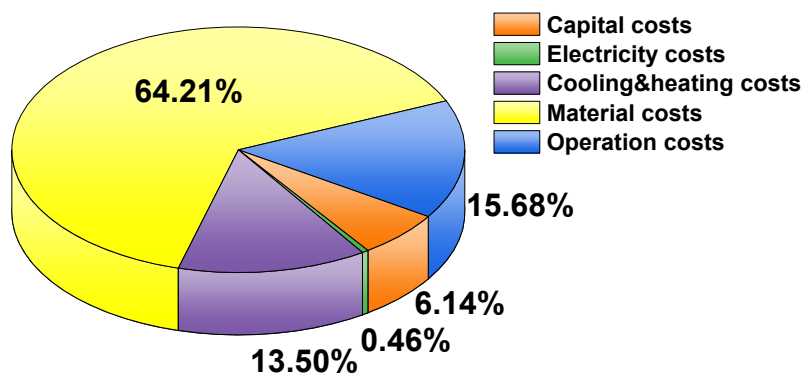

Figure S16. Contribution of each component to costs.

Table S15. Techno-economic analysis results.

Projects	Values, $/t
Capital costs	**77.90**
Equipment cost	163.14
Total Installed cost	238.80
Total plant cost	602.90
Total capital requirement	663.19
Electricity costs	**5.86**
Cooling&heating costs	**171.24**
Cooling water	7.37
Refrigerant - Freon 12	5.46
Steam @100PSI	158.40
Material costs	**814.59**
Hydrogen	45.80
Water	1.28
Propylene	713.83
Methanol	53.68
Operation costs	**198.96**
PO cost	1268.54

2.1.2. Life cycle assessment

The LCA boundary of the conventional PO production process is depicted in Figure S17. Emission factors involved in the LCA calculations are listed in Table S10. The LCA results for various scenarios are provided in Table S16. Moreover, Figure S18 compares the carbon footprints of the conventional PO production process and electrochemical PO production process.
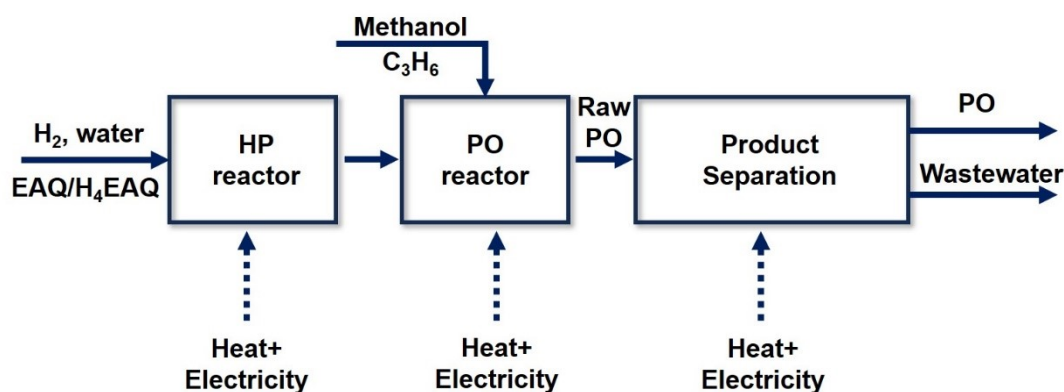

Figure S17. The system boundary of LCA in the conventional PO production process.

Table S16. LCA results for different scenarios.

Contributors	Scenario 1	Scenario 2	Scenario 3	Scenario 4	Scenario 5
Electricity (reaction)	0.043	0.043	0.001	-0.005	-0.005
Energy (separation)	1.823	1.823	1.823	1.823	0.000
Feedstocks	2.668	2.098	1.653	-0.601	-0.601
Hydrogen	1.054	0.484	0.040	-0.213	-0.213
Propylene	1.171	1.171	1.171	-0.241	-0.241
Methanol	0.443	0.443	0.443	-0.147	-0.147
[a] Wastewater	0.751	0.751	0.516	0.516	0.516
Total (kgCO$_2$e/kgPO)	4.535	3.965	3.477	1.218	-0.605

[a] Compared with other contributors, the carbon footprint unit for wastewater process is expressed as kgCO$_2$e/tPO.

Figure S18 compares the carbon footprints of electrochemical and conventional processes across five scenarios. Generally, the carbon footprint mainly depends on the energy and material supply of the processes. In Scenario 1, the electrochemical process exhibits a higher carbon footprint at 5.524 kgCO$_2$e/kgPO compared to the conventional

process (4.535 kgCO$_2$e/kgPO). This difference is attributed to the electrochemical process relying more on grid electricity in Scenario 1, while the conventional process has a lower dependency on electricity. In Scenario 3, the carbon footprint of the electrochemical process product is 2.737 kgCO$_2$e/kgPO, which is significantly lower than the conventional process (3.477 kgCO$_2$e/kgPO). The primary reason is the utilization of wind power to replace grid supply in Scenario 3, consequently resulting in a lower carbon footprint for the electrochemical process.
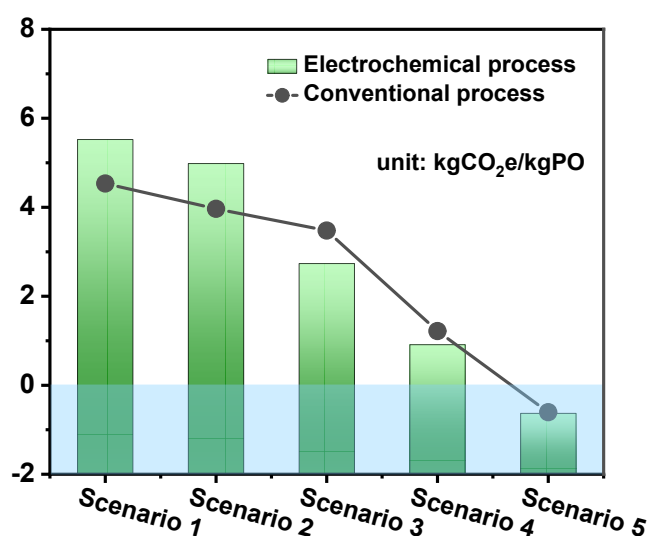

Figure S18. LCA comparisons for different scenarios.

As we all know, bio-based products are considered zero-carbon or even negative-carbon. By integrating bio-based materials or electricity alternatives, such as bio-electricity, bio-propylene, bio-hydrogen, and bio-methanol, into the existing PO production process, the carbon footprint can be substantially reduced. Hence, in Scenario 4, the electrochemical process achieves an exceptionally low carbon footprint of only 0.912 kgCO$_2$e/kgPO, due to the replacement with bio-based alternatives. However, it is essential to note that the promising results in practical scenarios currently face challenges because of techno-economic constraints in biomass energy development. Moreover, across Scenarios 1-4, the primary energy supply (thermal utility) in the entire process is mainly driven by natural gas. The prospect of achieving

a carbon-negative footprint for PO production becomes conceivable by substituting natural gas with zero-carbon alternatives such as biomass energy or zero-carbon electricity, see Scenario 5 in Figure S18. Nevertheless, it is imperative to note that realizing this promising target requires not only a stable renewable energy infrastructure but also the integration of reaction facilities tailored to match sustainable energy sources.

References

1. E. Zhao, G. Xia, Y. Li, J. Zhan, G. Yu and Y. Wang, *ACS EST Engg.*, 2023, **3**, 1800-1812.

2. Y. Liao, S.-F. Koelewijn, G. Van den Bossche, J. Van Aelst, S. Van den Bosch, T. Renders, K. Navare, T. Nicolaï, K. Van Aelst, M. Maesen, H. Matsushima, J. M. Thevelein, K. Van Acker, B. Lagrain, D. Verboekend and B. F. Sels, *Science*, 2020, **367**, 1385-1390.

3. E. Zhao, G. Xia, Y. Li, J. Zhan, G. Yu and Y. Wang, *ACS ES&T Engineering*, 2023, **3**, 1800-1812.

4. L. Liu, P. Jiang, H. Qian, L. Mu, X. Lu and J. Zhu, *Appl. Energy*, 2022, **311**, 118685.

5. P. Jiang, G. Zhao, L. Liu, H. Zhang, L. Mu, X. Lu and J. Zhu, *Bioresour. Technol.*, 2022, **351**, 127004.

6. P. Jiang, G. Zhao, H. Zhang, T. Ji, L. Mu, X. Lu and J. Zhu, *Green Energy Environ.*, 2022, DOI: 10.1016/j.gee.2022.12.004.

7. P. Jiang, L. Li, G. Zhao, H. Zhang, T. Ji, L. Mu, X. Lu and J. Zhu, *Chem. Eng. Sci.*, 2023, **276**, 118823.

8. P. Jiang, H. Zhang, G. Zhao, L. Li, T. Ji, L. Mu, X. Lu and J. Zhu, *Chin. J. Chem. Eng.*, 2024, DOI: 10.1016/j.cjche.2023.12.017.

9. P. De Luna, C. Hahn, D. Higgins, S. A. Jaffer, T. F. Jaramillo and E. H. Sargent, *Science*, 2019, **364**, eaav3506.

10. Y. Luo, K. Xie, P. Ou, C. Lavallais, T. Peng, Z. Chen, Z. Zhang, N. Wang, X.-Y. Li, I. Grigioni, B. Liu, D. Sinton, J. B. Dunn and E. H. Sargent, *Nature Catalysis*, 2023, **6**, 939-948.

11. Q. Yue, S. Li, X. Hu, Y. Zhang, M. Xue and H. Wang, *Energy Technology*, 2019, **7**, 1900365.

12. J. Diab, L. Fulcheri, V. Hessel, V. Rohani and M. Frenklach, *International Journal of Hydrogen Energy*, 2022, **47**, 25831-25848.

13. R. Nomura, N. Iki, O. Kurata, M. Kawabata, A. Tsutsumi, E. Koda and H. Furutani, 2011.

14. Z. Qin, G. Zhai, X. Wu, Y. Yu and Z. Zhang, *Energy Conversion and Management*, 2016, **124**, 168-179.

15. J. Streeck, C. Hank, M. Neuner, L. Gil-Carrera, M. Kokko, S. Pauliuk, A. Schaadt, S. Kerzenmacher and R. White, *Green Chem.*, 2018, **20**, 2742-2762.

16. R. Kajaste-Rudnitskaja, M. Hurme and P. Oinas, *Aims Energy*, 2018, **6**, 1074-1102.

17. M. Ghanta, D. R. Fahey, D. H. Busch and B. Subramaniam, *ACS Sustainable Chemistry & Engineering*, 2013, **1**, 268-277.

18. T. Liu, X. Meng, Y. Wang, X. Liang, Z. Mi, X. Qi, S. Li, W. Wu, E. Min and S. Fu, *Industrial & engineering chemistry research*, 2004, **43**, 166-172.

19. F. Yang, J. C. Meerman and A. P. C. Faaij, *Renewable and Sustainable Energy Reviews*, 2021, **144**, 111028.